CrossMark

Characterization and study on the thermal aging behavior of palladium–alumina catalysts

Aleksey A. Vedyagin[1,2] (iD) · Alexander M. Volodin[1] · Roman M. Kenzhin[1] ·
Vladimir O. Stoyanovskii[1] · Vladimir A. Rogov[1,3] · Dmitrii A. Medvedev[1] ·
Ilya V. Mishakov[1,2]

Abstract A series of Pd/Al_2O_3 catalysts were prepared by incipient wetness impregnation method. Palladium loading was varied in a range of 0.125–4.0 mass%. The catalytic performance of the samples was tested in model reaction of CO oxidation at oxygen excess. Catalysts were characterized by temperature-programmed reduction (TPR), electron paramagnetic resonance, and UV–visible spectroscopy. Thermal aging of chosen samples was performed at 1000 °C. The thermal aging behavior was studied using TPR, X-ray diffraction analysis, transmission electron microscopy, and X-ray photoelectron spectroscopy (XPS). It was shown that palladium stabilized in the form of dispersed surface Pd^{2+} species when Pd loading is 0.5 mass% and below. Samples with higher loading preferentially contain nanosized Pd particles. Agglomeration of Pd species during thermal aging was found to take place starting from Pd concentration of 1.0 mass%. In some cases, size of Pd particles exceeds 150 nm, which is in about 40 times higher comparing with the initial samples. According to XPS data, degree of Pd^{2+}-alumina interaction in the aged samples is also increased.

✉ Aleksey A. Vedyagin
vedyagin@catalysis.ru

1 Boreskov Institute of Catalysis, Novosibirsk, Russian Federation 630090

2 National Research Tomsk Polytechnic University, Tomsk, Russian Federation 634050

3 Novosibirsk State University, Novosibirsk, Russian Federation 630090

Introduction

Palladium supported on alumina is known to be one of the most intensively studied catalytic systems [1–7]. It attracts attention of the researchers due to its activity in hydrogenation of organic acids [1] and oils [8], hydrogenation and hydrodechlorination halogen-substituted organic/nitroorganic compounds [2, 6, 9], selective hydrogenation of polyunsaturated hydrocarbons [7], bromoallylation of phenylacetylene [3], ethylene selective hydrogenation [10] and acetoxylation [11], reduction in aromatic nitro compounds to amino compounds [4], and so on. In terms of environmental science, palladium–alumina catalysts were shown to be efficient in both gaseous (purification of exhaust and waste gases [12–21]) and liquid (treatment of contaminated waters [22]) media. Among gas-phase processes, catalytic oxidation of CO [12, 13, 16, 17, 21] and hydrocarbons [12, 14, 18–20, 23] seems to be of great importance.

Alumina due to its high thermal stability traditionally was used as a support for autocatalysts providing developed surface area for dispersing the active components [24, 25]. The use of the support with high surface area allows one to decelerate the process of active component agglomeration taking place at elevated temperatures [26]. At the same time, the nature of the support also affects the activity of the catalyst [27]. Thus, supports with oxygen storage capacity (CeO_2 and TiO_2) promote the oxygen activation for CO oxidation [28–30]. However, this function is the most actual in the case of three-way catalysts when the gas-phase oxygen is not in plenty. Contrary, when the thermal stability is more preferable (for example, in the case of diesel oxidation catalysis), alumina is considered as the most appropriate support. In addition, the thermal resistance of alumina-based catalysts can be easily

enhanced by changing the preparation method [31] or by doping the material with additives of different nature [15, 16, 18, 32].

The activity of palladium catalysts in oxidation processes is known to be strongly dependent on the dispersity of Pd species and its interaction with the support [33–36]. Character of interaction with the support, in its turn, is affected by the loading of active component and environment of catalyst's treatment [37–39]. All it determines the oxidative state of palladium to be stabilized. In terms of dispersity, the nature of Pd precursor used for the catalyst preparation plays a defining role [33, 34]. Chlorine-containing precursors are known to facilitate the formation of palladium species in the most dispersive form. Unfortunately, the presence of chlorine in composition of the final catalyst significantly decreases it activity. Pd nitrate (or corresponding nitrate-containing complexes) was shown to form the Pd species with acceptable dispersity and superior activity [34].

Another important point while studying the Pd/alumina catalysts is their behavior during the thermal aging treatment [36, 40–44]. Temperature of the procedure and environmental conditions are parameters defining the physicochemical and catalytic properties of the aged catalyst in most cases. When the temperature exceeds 1000 °C, phase transformation of alumina (an increase in α-phase content) as well as reduction in pore volume, specific surface area, and palladium dispersity occurs, thus resulting in sharp decrease in catalytic activity [10, 13, 26, 45]. Among the most important reasons of deactivation, strong metal-support interaction including Pd particles decoration with alumina and Pd particles agglomeration should be emphasized [26, 31, 45].

Recently, we have shown [44] that palladium species can be stabilized on a surface of γ-alumina when the Pd loading is 1 mass% or less. It corresponds to the concentration of electron donor sites on Al_2O_3 estimated using spin probe method based on electron paramagnetic resonance (EPR). In the present research, we have studied a series of Pd/γ-Al_2O_3 samples with Pd loading varied in a range of 0.125–4.0 mass% by means of developed EPR-based approach as well as by temperature-programmed reduction (TPR), and UV–visible spectroscopy. The effect of thermal aging treatment was elucidated using TPR, X-ray diffraction analysis, transmission electron microscopy, and X-ray photoelectron spectroscopy. The goal of the present work is to show the possibility of Pd/alumina catalysts preparation using palladium nitrate as a precursor with improved stability toward drastic thermal aging conditions. Isolated surface Pd^{2+} species appeared at Pd loading of 0.5 mass% and below were revealed to be responsible for appropriate activity and stability.

Experimental

Synthesis of the catalysts

The samples were prepared by incipient wetness impregnation of γ-Al_2O_3 (Condea) with aqueous solution of palladium nitrate. Prior to the impregnation, alumina grains were crushed, sieved to particle size of 0.25–0.5 mm, and calcined at 700 °C for 12 h (SSA = 188 m^2 g^{-1}). Different concentrations of palladium precursor in the impregnation solution were used to obtain the targeted Pd loading (0.125–4 mass%). After impregnation, the samples were dried in air at room temperature overnight. Then, the samples were dried at 110 °C for 12 h, heated in air up to 600 °C at 2 °C min^{-1} rate, and kept at 600 °C for 12 h. Catalyst aging was carried out isothermally at 1000 °C during 14 h with the fixed bed reactor. The aging gas composition was 10% water vapors in air.

Characterization of the samples

Investigation of the samples (100 mg, fraction of 0.25–0.5 mm) by means of temperature-programmed reduction (TPR) was carried out in a flow reactor system equipped with a thermal conductivity detector [44]. Low-temperature trap (T ≤ −50 °C) was placed between reactor and detector to remove water vapors released during the reduction in oxide phases. Prior to the testing, all samples were treated in oxygen atmosphere at 400 °C for 0.5 h followed by cooling down to −10 °C. Then, the reactor was flushed with Ar flow, and the testing procedure was started. The flow rate of reduction mixture (10% H_2 in Ar) was 40 mL min^{-1}. All samples were heated in the temperature range from −10 to 400 °C with the ramping rate of 10 °C min^{-1}.

Electron paramagnetic resonance (EPR) spectroscopy with spin probes was applied to characterize the donor sites of γ-Al_2O_3 support and Pd/γ-Al_2O_3 catalysts. The radical anions of 1,3,5-trinitrobenzene (TNB) were used as spin probes. The experimental procedure was similar to that reported in our recent publications [44, 46, 47]. A quartz sample tube with 20 mg of loaded catalyst sample was placed in a muffle furnace and heated on air at 500 °C for 12 h. Then, the sample was cooled down to room temperature and inundated with 2×10^{-2} M solution of TNB in toluene. At these conditions, the formation of TNB radical anions had started.

UV–Vis diffuse reflectance spectra were recorded between 200 and 850 nm using a UV–Vis spectrometer UV–Vis 2501 PC (Shimadzu) with IRS-250A diffusion reflection attachment. The reference for the all experiments was the support of the catalysts. The UV–Vis spectra were transformed into the Kubelka–Munk function F(R) [48].

The phase composition of the samples was studied in 2θ range 10°–75° on a Shimadzu XRD-7000 diffractometer (CuKα radiation, Ni filter on the reflected beam, and a scintillation detector with amplitude discrimination). Interpretation of the diffraction patterns was done in accordance with JCPDS-ICDD database [49].

Transmission electron microscopy (TEM) images were obtained using a JEOL JEM-2010 electron microscope with lattice resolution 0.14 nm at accelerating voltage 200 kV. The local energy-dispersive X-ray (EDX) micro-analysis was carried out using EDAX spectrometer with energy resolution 127 eV.

The X-ray photoelectron spectra (XPS) were obtained with a VG ESCA-3 (VG Scientific, GB) electron with Mg Kα radiation. The binding energy of adventitious C1 s (284.5 eV) was used as an internal reference. The pressure in the analysis chamber was maintained lower than 1×10^{-7} mbar. Energy regions were selected after a general survey and scanned with several sweeps until a good signal-to-noise ratio was observed. The accuracy of the binding energy (BE) values was $\pm$ 0.1 eV.

Testing the catalytic activity

The catalytic performance of samples in a model reaction of CO oxidation was studied using laboratory-scale light-off testing procedure. After grinding and sieving to reach the grain size in the range of 0.25 to 0.5 mm, catalyst samples were employed for testing. The feed stream consisted of 0.15 vol% CO, 14 vol% O_2, 0.01 vol% NO, 5 vol% H_2O, and N_2 as the balance. The total gas flow was 0.3 dm^3 min^{-1} corresponding to a feed gas space velocity (GHSV) of 180,000 h^{-1}. The temperature of the catalyst was increased from 60 to 320 °C with a heating rate of 10 °C min^{-1}. The gas concentrations were determined using FTIR gas analyzer (Siemens). Each sample was tested in several heating–cooling cycles.

The turnover frequency (TOF), number of molecules of CO converted per surface atom of palladium particles and per second, was calculated for all samples at 120 °C as described in Ref. [50].

Results and discussion

Characterization of the prepared samples

As it was mentioned, Pd/Al$_2$O$_3$ catalysts are widely used in vehicle pollution control systems in order to oxidize CO and hydrocarbons. Typical light-off curves of CO conversion versus temperature for a number of catalysts with various Pd loadings are shown in Fig. 1. Presented data are related to the first cycle of catalytic reaction, before which

the catalyst sample was maintained in the reaction gas feed at 60 °C for 1 h. The monotonous dependence of the T50 parameter (temperature corresponding to 50% of CO conversion) upon Pd concentration can be obviously seen. This dependence was found to reach its plateau at the Pd concentration of about 0.5%. Further increase for palladium deposited on alumina has no effect on T50. Figure 2 shows light-off curves (three consecutive cycles) for fresh and thermally aged 1.0%Pd/Al$_2$O$_3$ catalyst, as an example. Data for all samples are summarized in Table 1. There are two important notes, which could be made based on results presented in Figs. 1 and 2, and Table 1. Firstly, method of catalytic testing is very sensitive since it allows one to detect reliably the active sites of Pd/Al$_2$O$_3$ catalysts at low Pd loading. Secondly, the catalytic performance of x%Pd/Al$_2$O$_3$ samples does not practically improve when x% exceeds 0.5%. Therefore, the samples with Pd loading of 0.5 mass% and below are believed to be relatively stable and resistant toward high-temperature agglomeration. In order to clarify this assumption, the catalysts were characterized by a set of physicochemical methods.

Temperature-programmed reduction (TPR) by hydrogen appears to be a useful and highly sensitive method for detection and quantitative definition of coarse particles of PdO phase dispersed on the surface of Pd-containing oxide catalysts [51–53]. It is caused by rather narrow temperature range around 20 °C in which the sample absorbs hydrogen due to reduction of PdO and formation of Pd hydride [54]. Unstable Pd hydride undergoes decomposition near 90 °C which is indicated by the hydrogen release peak on TPR curve. TPR profiles for a series of studied Pd/Al$_2$O$_3$ catalysts with various contents of the supported Pd are presented in Fig. 3.
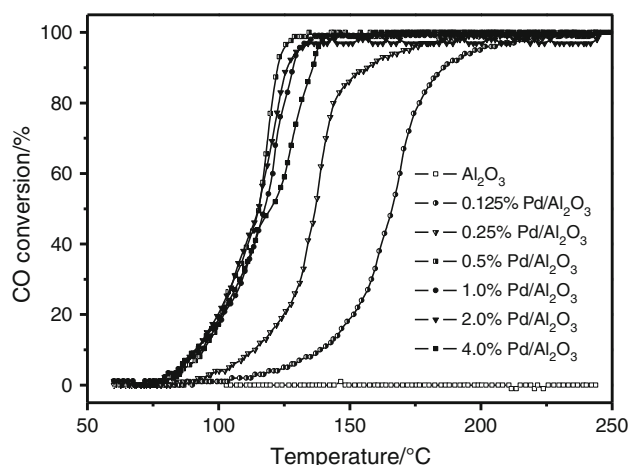

Fig. 1 Temperature dependences of the CO conversion for the x%Pd/Al$_2$O$_3$ samples with various concentrations of supported Pd. Data are provided for the first catalytic cycle
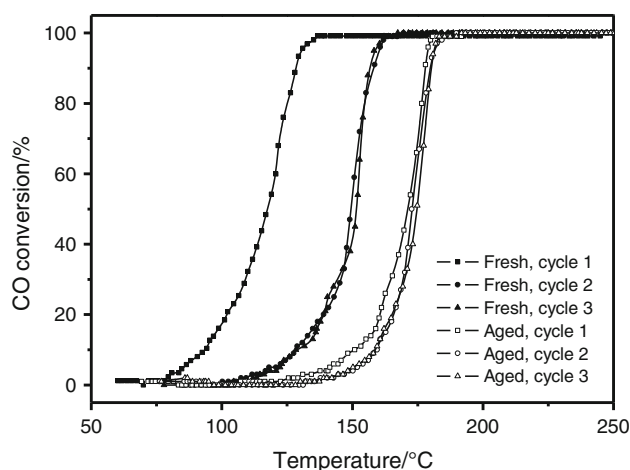
Fig. 2 Temperature dependences of the CO conversion for the fresh and thermally aged 1.0%Pd/Al$_2$O$_3$ sample in three consecutive catalytic cycles

Fig. 3 TPR profiles for Pd/Al$_2$O$_3$ catalysts with various Pd loadings. Prior to measurements, all the samples were calcined in oxygen flow at 400 °C

In general, the obtained TPR results are in good correlation with the data on Pd/Al$_2$O$_3$ catalysts available in the literature [51–53]. The presence of three characteristic areas of hydrogen consumption (A, B, and C) is readily shown in Fig. 3. The first low-temperature sharp peak (A) around 20 °C emerges for samples containing more than 1% of supported Pd and gives primary contribution to the total hydrogen uptake for sample 4%Pd/Al$_2$O$_3$ while it remains negligible for low-content Pd/Al$_2$O$_3$ samples (Table 2). According to the literature data, this peak can be attributed to consumption of hydrogen by PdO particles. The wide peak (B) having an uptake maximum at a range of 120–150 °C keeps rising with the increase in Pd concentration up to 2%, but then practically disappears for 4%Pd/Al$_2$O$_3$ sample (Fig. 3; Table 2). The high-temperature peak (C) characterized with H$_2$ uptake maximum around 300–320 °C was found to be prevailing for a sample containing 0.125% Pd (Fig. 3, curve 2) and virtually reveals no further intensity growth at the Pd concentration increase up to 4% (Table 2).

It is worth noting that the total hydrogen uptake measured in the temperature range from −10 to +400 °C and
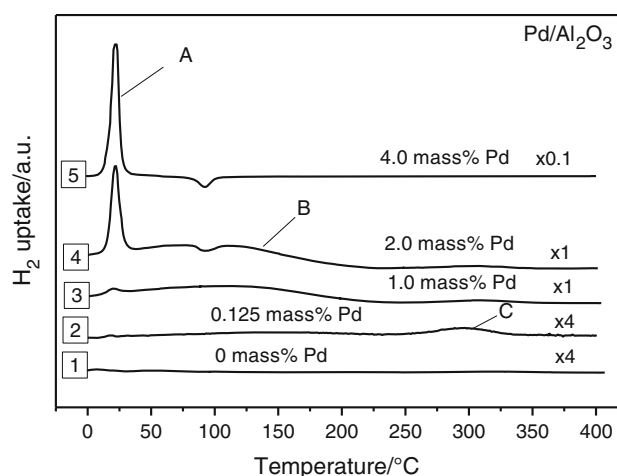
calculated by combining the (A), (B), and (C) peak intensities coincides for all samples with the total amount of Pd atoms in a sample within experimental accuracy (Table 2). So, almost entirely supported Pd in the studied samples exists in the ionic form Pd^{2+}. At the same time, an increase in Pd loading leads to the changes of the contribution of PdO phases with different reducibility.

The series of x%Pd/Al$_2$O$_3$ samples (where $x < 1\%$) indicating the absence of the PdO phase (exhibiting no peak (A) on TPR curve, accordingly) represent the greatest interest within the scope of present research and results on EPR spin probes method. As it was shown in our papers [44, 46, 47], the spin probe method represents an effective tool for investigation of the active sites present in Pd/Al$_2$O$_3$ and Pd-Rh/Al$_2$O$_3$ catalysts characterized with low content of the supported precious metals. The important role of the intrinsic donor sites of the Al$_2$O$_3$ support in stabilization of surface Pd^{2+} species was demonstrated.

In the present research, the samples with different Pd loading were activated at 500 °C and then inundated with 2×10^{-2} M solution of TNB in toluene. The reaction of radical formation was conducted at 80 °C. Concentration

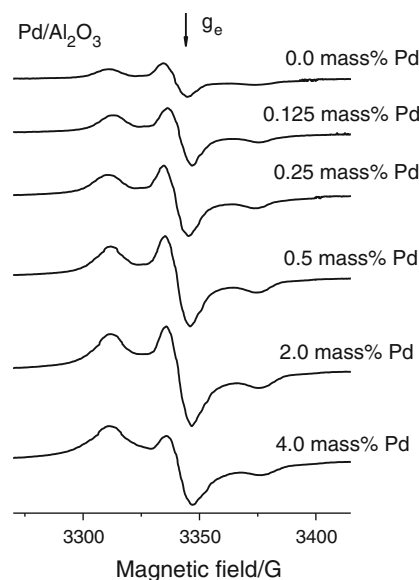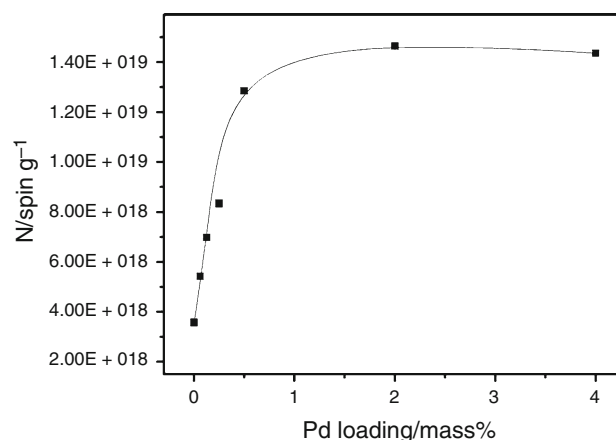**Table 1** Catalytic performance of x%Pd/Al$_2$O$_3$ samples in CO oxidation

Pd loading/ mass%	T50 (fresh samples)/°C			TOF/s^{-1}	T50 (aged samples)/°C		
	First cycle	Second cycle	Third cycle		First cycle	Second cycle	Third cycle
0.125	166	169	174	0.001	179	181	181
0.25	137	150	156	0.027	173	173	175
0.5	115	129	131	0.116	149	153	155
1	118	150	152	0.069	171	173	175
2	115	143	147	0.060	169	174	173
4	120	151	155	0.036	175	179	180

Table 2 Hydrogen uptake calculated from TPR data measured for Pd/Al$_2$O$_3$ samples with various Pd loadings

Pd loading/ mass%	N(Pd)/ μMol g^{-1}	H$_2$ uptake, N(H$_2$)/μMol g^{-1}				N(H$_2$)/ N(Pd)
		Peak A	Peak B	Peak C	Sum A + B + C	
0	0	<0.1	<1.5	<1	<2.6	–
0.125	11.7	<0.1	5.2	3.6	8.9	0.76
0.5	47.0	1.5	37	2.8	41.3	0.88
1	94.0	2.5	93	5.6	101.1	1.07
2	188	41	173	5.2	219.2	1.17
4	376	470	6	7.2	483	1.28

Fig. 5 Concentration of TNB anion radicals resulting from adsorption of 1,3,5-trinitrobenzene (TNB) over Pd/Al$_2$O$_3$ catalyst versus Pd loading

of radicals was registered after 5 h. The resulted EPR spectra are presented in Fig. 4. It is seen that the intensity of signal increases with regard to Pd loading. Figure 5 demonstrates how concentration of anion radicals depends on content of palladium. As evident, the concentration grows until the Pd loading of 0.5 mass% and then reaches its plateau. Note that this observation is in similar to results of catalytic tests described above.

It can be suggested that the strong bonding of isolated Pd^{2+} species with the donor site prevents their agglomeration with formation of PdO particles. Pd^{2+} species therefore prefer being stabilized, first of all, on the donor sites of Al$_2$O$_3$. As soon as all donor sites are occupied (when Pd concentration exceeds 0.5 mass%), the nucleation of PdO nanoparticles statistically distributed throughout the surface begins to take place. The values of
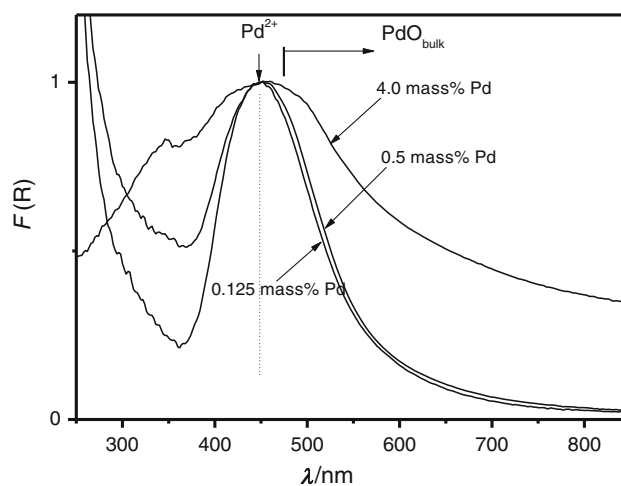
turnover frequency calculated at 120 °C (Table 1) start to decrease at Pd loading of 1.0 mass% and above.

The revealed effect of the intrinsic donor sites of oxide support on stabilization of the isolated Pd^{2+} species is in a good agreement with the results of quantum chemical calculations made for Pd/MgO system [55] where the important role of electron donor sites of MgO in stabilization of Pd^{2+} species was demonstrated.

UV–Vis diffuse reflectance (DR) spectra for 0.125–4.0% Pd/Al$_2$O$_3$ samples calcined at 600 °C are presented in Fig. 6. It seems possible to separate two typical areas by concentration of supported metal characterized by different state of Pd (0.125–0.5 and 0.5–4.0%).

At low Pd loading (0.125–0.5 mass%, Fig. 6), the Pd^{2+} species were found to be isolated. Their UV–visible spectra show a d–d transition at 450 nm and palladium–oxygen

Fig. 4 EPR spectra recorded after adsorption of 1,3,5-trinitrobenzene on Al$_2$O$_3$ and Pd/Al$_2$O$_3$ samples

Fig. 6 DR UV–Vis spectra of Pd/Al$_2$O$_3$ (600 °C, 0.125–4.0 mass% of Pd). The arrows show the lines corresponding to the d–d transitions of Pd$_s^{2+}$ and the spectral region characterizing the appearance of PdO particles

charge transfer band at 250 nm [56, 57]. At high Pd loading (4.0 mass%, Fig. 6), with an increase in the PdO particle size, the formation of absorption edge of band gap (E_g) at a higher wavelength than the d–d transition of isolated Pd^{2+} species takes place. This makes it possible to evaluate the average particle size of PdO. Such size characterization is based on the relation between the domain size and the band gap energy (E_g) of a semiconductor [58]. Bulk band gap energy of PdO is about 0.8 eV [59]. With the increase in the Pd content from 0.5 to 4.0%, the band gap of PdO particles decreases from 2.35 to 2.0 eV.

Studying the thermal aging behavior of palladium species

In order to study the thermal aging effect at elevated temperature, three Pd-containing samples were chosen. Samples 0.125%Pd/Al$_2$O$_3$ and 2%Pd/Al$_2$O$_3$ represent low-loaded and high-loaded catalysts, respectively. Sample 0.5%Pd/Al$_2$O$_3$ was selected as a medium one. Each sample was characterized with a different technique in accordance with the sensitivity of the methods and usability of obtaining information.

Data concerning the effect of the thermal aging procedure on the ratio of TPR peaks (A), (B), and (C) for 0.5%Pd/Al$_2$O$_3$ sample are presented in Table 3. The significant increase in contribution of peak (A) in total H$_2$ uptake after calcination of the samples at 1000 °C accompanied with substantial reduction in peak (B) intensity is well seen. At the same time, the total consumption of hydrogen after thermal aging of sample in air at 1000 °C does not practically change (Table 3). A quite noticeable growth of peak (C) contribution into total hydrogen uptake in the considered temperature range (under 400 °C) should be noted as well.

The low- and medium-loaded samples were examined by means of EPR. Figure 7 shows corresponding diagram. Concentrations of donor sites for pure alumina calcined at the same temperatures are given for comparison. As follows from the data, calcination at 1000 °C slightly decreases the intensity of EPR signal in all cases. The
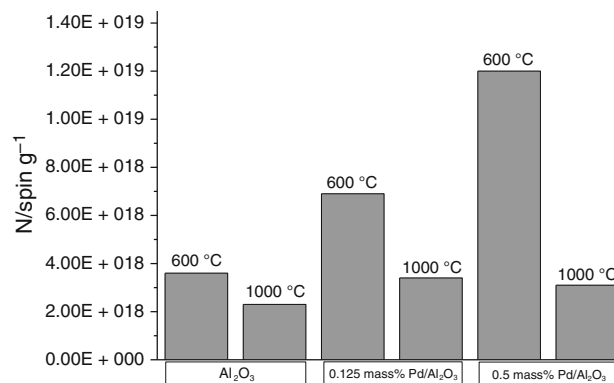

Fig. 7 Concentration of donor sites on Al$_2$O$_3$, 0.125%Pd/Al$_2$O$_3$, and 0.5%Pd/Al$_2$O$_3$ samples calcined at 600 °C and 1000 °C

reduction in anion radical concentration corresponds to decreased amount of donor sites on the surface of the support. The observed result is connected with alumina phase transformation only. No palladium species agglomeration or strengthened interaction with support takes place in this case. Thus, low-loaded Pd-containing samples can be considered as thermally stable catalysts, at least up to the temperature of alumina phase transformation (about 1000 °C).

The evidence of alumina phase transformation can be confirmed by XRD data. Samples 2%Pd/Al$_2$O$_3$ and pure alumina calcined at 600 and 1000 °C were comparatively studied by this technique. As shown in Table 4, for the samples heated at 600 °C, the γ-Al$_2$O$_3$ phase is identified. Palladium in 2%Pd/Al$_2$O$_3$ sample is represented by PdO particles with tetragonal structure and RCS (region of coherent scattering) of 4 nm. The thermal aging treatment (1000 °C) results in transformation of γ-Al$_2$O$_3$ into α-Al$_2$O$_3$ and δ-Al$_2$O$_3$ phases. Noticeable agglomeration of

Table 3 Hydrogen uptake calculated from TPR data measured for 0.5%Pd/Al$_2$O$_3$ catalyst: the initial sample (heated at 600 °C) and thermally aged sample (air, 1000 °C, 12 h)

T/°C	N(Pd)/ μMol g^{-1}	H$_2$ uptake, N(H$_2$)/μMol g^{-1}				N(H$_2$)/ N(Pd)
		Peak A	Peak B	Peak C	Sum A + B + C	
600	47.0	1.5	37	2.8	41.3	0.88
1000	47.0	12	19	9.6	40.6	0.86

Table 4 XRD data for Al$_2$O$_3$ and 2%Pd/Al$_2$O$_3$ samples

Sample	Phase composition	Unit cell parameter/nm	RCS/ nm
γ-Al$_2$O$_3$ (600 °C)	γ-Al$_2$O$_3$	0.7915(5)	5.0
γ-Al$_2$O$_3$ (1000 °C)	α-Al$_2$O$_3$ (∼65%)	–	–
	δ-Al$_2$O$_3$ (∼35%)	0.7870(5)	11.0
2%Pd/γ-Al$_2$O$_3$ (600 °C)	PdO (tetr.)	–	4.0
	γ-Al$_2$O$_3$	0.7915(5)	5.0
2%Pd/γ-Al$_2$O$_3$ (1000 °C)	PdO (tetr.)	–	35.0
	α-Al$_2$O$_3$ (∼65%)	–	–
	δ-Al$_2$O$_3$ (∼35%)	0.7865(5)	–
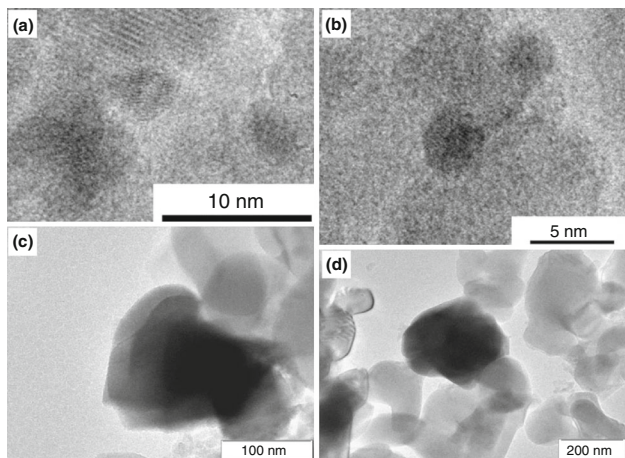
Fig. 8 TEM images of PdO particles for 2%Pd/Al$_2$O$_3$ sample calcined at 600 °C (**a**, **b**) and 1000 °C (**c**, **d**)
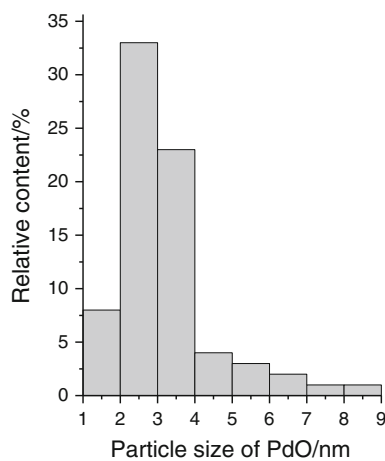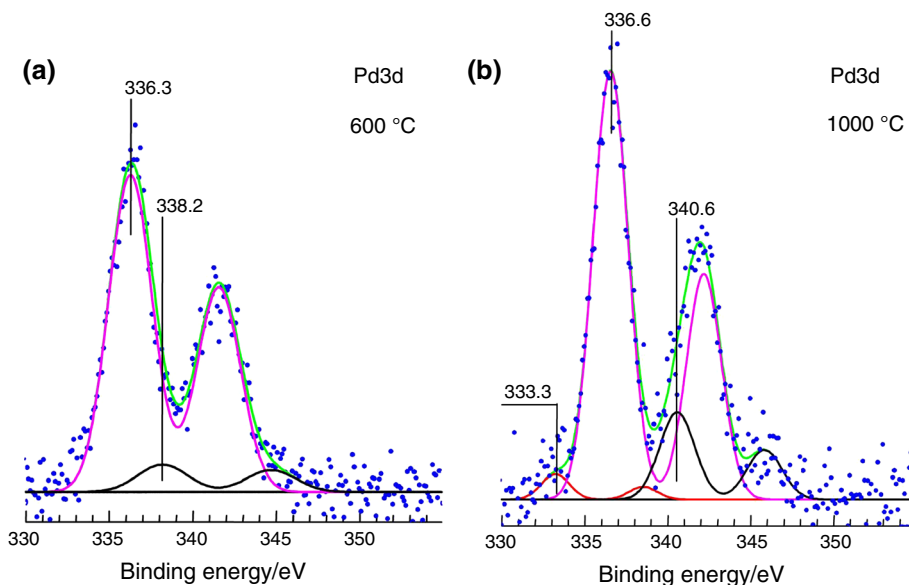

Fig. 9 PdO particle size distribution for the 2%Pd/Al$_2$O$_3$ sample calcined at 600 °C

Fig. 10 XPS spectra of Pd3d for 2%Pd/Al$_2$O$_3$ sample calcined at 600 °C (**a**) and 1000 °C (**b**)

PdO particles takes place during the treatment (increasing of RSC from 5 to 35 nm).

According to results of TEM study for 2%Pd/Al$_2$O$_3$ sample presented in Figs. 8 and 9, PdO particle size distribution appears to be quite uniform with the maximum at 2–4 nm when the sample was treated at 600 °C. However, as it follows from TEM images (Fig. 8a, b), the structure of the particles is not regular in many cases. Unfortunately, it was not possible to calculate the particle size distribution for the sample heated at 1000 °C. The size of PdO particles in this sample exceeds 150–200 nm (Fig. 8c, d). It should be mentioned that enlargement of PdO particles from few nanometers up to hundreds of nanometers as a result of high-temperature agglomeration was also reported in Refs. [41, 43, 45].

Sample 2%Pd/Al$_2$O$_3$ calcined at 600 °C and 1000 °C was also characterized by XPS. Corresponding spectra of Pd3d region are shown in Fig. 10. As shown in Fig. 10 A, the sample calcined at 600 °C illustrates the presence of PdO species (336.3 eV). At the same time, according to the literature the binding energy for PdO is 336.8 eV. This difference can be attributed to formation of PdO particles with tetragonal structure confirmed by XRD. Peak with $E_b = 338.2$ eV may be refer to Pd^{2+} stabilized within the structure of Al$_2$O$_3$ (strengthening of Pd^{2+}-support interaction). In sample, calcined at 1000 °C the main part of palladium is represented by PdO species on the surface of support ($E_b = 336.6$ eV). A small parts of Pd^0 ($E_b = 333.3$ eV) as well as Pd^{2+} in the structure of the support ($E_b = 340.6$ eV) are observed.

Summarizing these results, it can be concluded that in the case of high-loaded Pd/alumina samples the intensive PdO particles agglomeration accompanied with strong metal-support interaction occurs. The strengthening of

Pd^{2+}-alumina interaction can be explained by decoration of PdO particles with alumina which is known to take place at temperature of 1000 °C and above [26, 45]. When the concentration of supported Pd is comparable with donor site concentration ($0.5\%Pd/Al_2O_3$), the effect of high-temperature aging is not so evident. Such catalysts can be considered as thermally quasi-stable systems. They undergo deactivation at elevated temperatures, but significantly slowly. And finally, the most efficient catalysts are the samples with low Pd loading (less than 0.5 mass%). These systems show high activity along with superior stability.

Conclusions

The role of atomically dispersed forms of supported precious metals for performance in various catalytic reactions is now intensively discussed in the literature. It is rather obvious that reduction in the particle size of supported metal (or its oxide) would lead to enhancement of its effectively working surface. At the same time, the shift from nanoparticles to the isolated species stabilized on the surface of the support is believed to make cardinal changes in its coordination environment and, as a consequence, to alter its reactivity. For Pd/Al_2O_3 system, this effect is convincingly demonstrated on quantitative level by means of TPR. The obtained results unambiguously indicated much higher stability of the isolated Pd^{2+} species with respect to hydrogen atmosphere as compared with PdO particles. Such isolated species are considered to be responsible for the high activity of Pd/Al_2O_3 system in the catalytic oxidation of CO.

It is necessary to emphasize that the presence of specific (donor) sites of the support is liable for stabilization of Pd^{2+} species in the case of low-loaded Pd/Al_2O_3 catalysts (0.125–0.5 mass%). The concentration of donor sites in Al_2O_3 support is rather low and was evaluated to be around $(1–2) \times 10^{19}$ sites g^{-1}. Taking into account the value of the specific surface area of support (about 200 m^2 g^{-1}), one can estimate the surface concentration of such sites to be near 10^{17} sites m^{-2}, i.e., less than 1% of a monolayer. It is also rather obvious that the appearance of such sites is caused by the presence of coordinately unsaturated structures on the surface. There are no unambiguous data in the literature regarding the structure of such sites so far. It seems reasonable to expect them to be present on a high-indexed faces of nanocrystals or on the edges and tops located between them.

In general, the obtained results can be considered as an indication of the possibility to create stable and highly active CO oxidation catalysts containing rather low concentrations of the supported Pd. An important role in the formation of the active sites of such catalysts is played by intrinsic sites of the support allowing one to stabilize the isolated Pd^{2+} species. The techniques developed for diagnostics of such sites permit one to make their preliminary selection from the point of view of task to be solved.

References

1. Hong UG, Hwang S, Seo JG, Yi J, Song IK. Hydrogenation of succinic acid to γ-butyrolactone over palladium catalyst supported on mesoporous alumina xerogel. Catal Lett. 2010;138:28–33.
2. Vishwanathan V, Jayasri V, Mahaboob Basha P. Vapor phase hydrogenation of o-chloronitrobenzene (o-CNB) over alumina supported palladium catalyst—a kinetic study. React Kinet Catal Lett. 2007;91:291–8.
3. Fukuyama T, Kippo T, Ryu I, Sagae T. Addition of allyl bromide to phenylacetylene catalyzed by palladium on alumina and its application to a continuous flow synthesis. Res Chem Intermed. 2009;35:1053.
4. Arora S, Kapoor P, Singla ML. Catalytic studies of palladium nanoparticles immobilized on alumina synthesized by a simple physical precipitation method. React Kinet Mech Catal. 2010;99:157–65.
5. Berenblyum AS, Podoplelova TA, Shamsiev RS, Katsman EA, Danyushevsky VY. On the mechanism of catalytic conversion of fatty acids into hydrocarbons in the presence of palladium catalysts on alumina. Pet Chem. 2011;51:336–41.
6. Gopinath R, Seshu Babu N, Vinod Kumar J, Lingaiah N, Sai Prasad PS. Influence of Pd precursor and method of preparation on hydrodechlorination activity of alumina supported palladium catalysts. Catal Lett. 2008;120:312–9.
7. Thomazeau C, Cseri T, Bisson L, Aguilhon J, Minh DP, Boissière C, Durupthy O, Sanchez C. Nano design of alumina supported monometallic catalysts: a promising way to improve the selective hydrogenation of poly-unsaturated hydrocarbons. Top Catal. 2012;55:690–9.
8. Cizmeci M, Musavi A, Tekin A, Kayahan M. Comparison of two palladium catalysts on different supports during hydrogenation. J Am Oil Chem Soc. 2006;83:1063–8.
9. Karpiński Z, d'Itri JL. Hydrodechlorination of 1,1-dichlorotetrafluoroethane on supported palladium catalysts. A static-circulation reactor study. Catal Lett. 2001;77:135–40.
10. Takht Ravanchi M, Fadaeerayeni S, Rahimi Fard M. The effect of calcination temperature on physicochemical properties of alumina as a support for acetylene selective hydrogenation catalyst. Res Chem Intermed. 2016;42:4797–811.
11. Voskanyan PS. Effect of the nature of a support on the catalytic activity of a palladium catalyst in the synthesis of vinyl acetate by gas-phase ethylene acetoxylation. Catal Ind. 2013;5:90–7.
12. Heck RM, Farauto RJ. Catalytic air pollution control: commercial technology. 2nd ed. New York: Wiley; 2002.
13. Zheng Q, Farrauto R, Deeba M. Part II: oxidative thermal aging of Pd/Al_2O_3 and $Pd/CexOy$-ZrO_2 in automotive three way catalysts: the effects of fuel shutoff and attempted fuel rich regeneration. Catalysts. 2015;5:1797–814.
14. Li M, Weng D, Wu X, Wan J, Wang B. Importance of re-oxidation of palladium by interaction with lanthana for propane combustion over Pd/Al_2O_3 catalyst. Catal Today. 2013;201:19–24.

15. Rashidzadeh M, Peyrovi MH, Mondegarian R. Alumina-based supports for automotive palladium catalysts. React Kinet Catal Lett. 2000;69:115–22.

16. Osaki T, Yamada K, Watari K, Tajiri K, Shima S, Miki T, Tai Y. Palladium–alumina cryogel with high thermal stability and CO oxidation activity. Catal Lett. 2012;142:95–9.

17. Meusel I, Hoffmann J, Hartmann J, Heemeier M, Bäumer M, Libuda J, Freund H-J. The interaction of oxygen with alumina-supported palladium particles. Catal Lett. 2001;71:5–13.

18. Chen L, Feng T, Wang P, Xiang Y, Ou B. Catalytic properties of Pd supported on hexaaluminate coated alumina in low temperature combustion of coal mine ventilation air methane. Kinet Catal. 2013;54:767–72.

19. Demoulin O, Navez M, Ruiz P. The activation of a Pd/γ-alumina catalyst during methane combustion: investigation of the phenomenon and of potential causes. Catal Lett. 2005;103:149–53.

20. Haack LP, Otto K. X-ray photoelectron spectroscopy of Pd/γ-alumina and Pd foil after catalytic methane oxidation. Catal Lett. 1995;34:31–40.

21. Weng X, Yuan X, Li H, Li X, Chen M, Wan H. The study of the active surface for CO oxidation over supported Pd catalysts. Sci China Chem. 2015;58:174–9.

22. Munakata N, Reinhard M. Palladium catalysis for the treatment of contaminated waters: a review. In: Smith JA, Burns SE, editors. Physicochemical groundwater remediation. New York: Kluwer Academic Publishers; 2002. p. 45–71.

23. Perdigón-Melón JA, Auroux A, Bonnetot B. Calorimetric study of methane interaction with supported Pd catalysts. J Therm Anal Calorim. 2003;72:443–51.

24. Twigg MV. Catalytic control of emissions from cars. Catal Today. 2011;163:33–41.

25. Li H, Zhu Q, Li Y, Gong M, Chen Y, Wang J, Chen Y. Effects of ceria/zirconia ratio on properties of mixed CeO2–ZrO2–Al2O3 compound. J Rare Earth. 2010;28:79–83.

26. Zheng T, He J, Zhao Y, Xia W, He J. Precious metal-support interaction in automotive exhaust catalysts. J Rare Earth. 2014;32:97–107.

27. Satsuma A, Osaki K, Yanagihara M, Ohyama J, Shimizu K. Activity controlling factors for low-temperature oxidation of CO over supported Pd catalysts. Appl Catal B-Environ. 2013;132–133:511–8.

28. Li K, Wang X, Zhou Z, Wu X, Weng D. Oxygen storage capacity of Pt-, Pd-, Rh/CeO2-based oxide catalyst. J Rare Earth. 2007;25:6–10.

29. Alikin EA, Vedyagin AA. High temperature interaction of rhodium with oxygen storage component in three-way catalysts. Top Catal. 2016;59:1033–8.

30. Widmann D, Behm RJ. Active oxygen on a Au/TiO2 catalyst: formation, stability, and CO oxidation activity. Angew Chem Int Ed. 2011;50:10241–5.

31. Fessi S, Ghorbel A. Preparation of alumina supported palladium catalysts by sol-gel method. J Sol-Gel Sci Technol. 2000;19:417–20.

32. Zheng X, Chen X, Chen J, Zheng Y, Jiang L. Synthesis and application of highly dispersed ordered mesoporous silicon-doped Pd-alumina catalyst with high thermal stability. Chem Eng J. 2016;297:148–57.

33. Wang Q, Li G, Zhao B, Zhou R. The effect of rare earth modification on ceria–zirconia solid solution and its application in Pd-only three-way catalyst. J Mol Catal A-Chem. 2011;339:52–60.

34. Haneda M, Kintaichi Y, Nakamura I, Fujitani T, Hamada H. Effect of surface structure of supported palladium catalysts on the activity for direct decomposition of nitrogen monoxide. J Catal. 2003;218:405–10.

35. Soni KC, Krishna R, Chandra Shekar S, Singh B. Catalytic oxidation of carbon monoxide over supported palladium nanoparticles. Appl Nanosci. 2016;6:7–17.

36. Légaré P, Finck F, Roche R, Maire G. Palladium particles growth on various aluminas. In: Chapon C, Gillet MF, Henry CR, editors. Small particles and inorganic clusters. Berlin: Springer; 1989. p. 19–22.

37. Shubin VE, Shvets VA, Savel'eva GA, Popova NM. EPR study of Pd+ ions in palladium–alumina catalysts and their interaction with carbon monoxide and oxygen. Kinet Catal. 1982;23:1153–60 (in Russian).

38. Sass AS, Shvets VA, Savel'eva GA, Popova NM, Kazanskii VB. EPR study of palladium and platinum ions in Pd/MgO and Pt/MgO catalysts. Kinet Catal. 1983;24:1167–72 (in Russian).

39. Sass AS, Shvets VA, Savel'eva GA, Popova NM, Kazanskii VB. Reactivity of O2− anion-radicals and mechanism of low-temperature oxidation of carbon monoxide on Ce/Al2O3 and Ce-Pd/Al2O3. Kinet Catal. 1985;26:924–31 (in Russian).

40. Chen X, Schwank JW, Fisher GB, Cheng Y, Jagner M, McCabe RW, Katz MB, Graham GW, Pan X. Nature of the two-step temperature-programmed decomposition of PdO supported on alumina. Appl Catal A-Gen. 2014;475:420–6.

41. Cao Y, Ran R, Wu X, Zhao B, Wan J, Weng D. Comparative study of ageing condition effects on Pd/Ce0.5Zr0.5O2 and Pd/Al2O3 catalysts: catalytic activity, palladium nanoparticle structure and Pd-support interaction. Appl Catal A-Gen. 2013;457:52–61.

42. Matam SK, Otal EH, Aguirre MH, Winkler A, Ulrich A, Rentsch D, Weidenkaff A, Ferri D. Thermal and chemical aging of model three-way catalyst Pd/Al2O3 and its impact on the conversion of CNG vehicle exhaust. Catal Today. 2012;184:237–44.

43. Misono M. Recent progress in the practical applications of heteropolyacid and perovskite catalysts: catalytic technology for the sustainable society. Catal Today. 2009;144:285–91.

44. Vedyagin AA, Volodin AM, Stoyanovskii VO, Mishakov IV, Medvedev DA, Noskov AS. Characterization of active sites of Pd/Al2O3 model catalysts with low Pd content by luminescence, EPR and ethane hydrogenolysis. Appl Catal B-Environ. 2011;103:397–403.

45. Zhou Y, Wang Z, Liu C. Perspective on CO oxidation over Pd-based catalysts. Catal Sci Technol. 2015;5:69–81.

46. Vedyagin AA, Gavrilov MS, Volodin AM, Stoyanovskii VO, Slavinskaya EM, Mishakov IV, Shubin YV. Catalytic purification of exhaust gases over Pd–Rh alloy catalysts. Top Catal. 2013;56:1008–14.

47. Vedyagin AA, Volodin AM, Stoyanovskii VO, Kenzhin RM, Slavinskaya EM, Mishakov IV, Plyusnin PE, Shubin YV. Stabilization of active sites in alloyed Pd–Rh catalysts on γ-Al2O3 support. Catal Today. 2014;238:80–6.

48. Boehm HP, Knözinger H. In: Anderson JR, Boudart M, editors. Catalysis-science and technology, vol. IV. Berlin: Springer; 1983. p. 39–209.

49. Powder Diffraction File. PDF-2/Release 2009: International Centre for Diffraction Data. USA.

50. Vedyagin AA, Volodin AM, Kenzhin RM, Chesnokov VV, Mishakov IV. CO Oxidation over Pd/ZrO2 catalysts: role of support's donor sites. Molecules. 2016;21:1289.

51. Lieske H, Volter J. Palladium redispersion by spreading of palladium(II) oxide in oxygen treated palladium/alumina. J Phys Chem. 1985;89:1841–2.

52. Lieske H, Lietz G, Hanke W, Völter J. Oberflächenchemie, Sintern und Redispergieren von Pd/Al2O3-Katalysatoren. Z Anorg Allg Chem. 1985;527:135–49.

53. Juszczyk W, Karpinski Z, Ratajczykowa I, Stanasiuk Z, Zielinski J, Sheu LL, Sachtler WMH. Characterization of supported palladium catalysts: III. PdAl2O3. J Catal. 1989;120:68–77.

54. Pawlonka J, Gac W, Greluk M, Słowik G. Application of microemulsion method for development of methanol steam reforming Pd/ZnO catalysts. J Therm Anal Calorim. 2016;125:1265–72.

55. Sicolo S, Pacchioni G. Charging and stabilization of Pd atoms and clusters on an electron-rich MgO surface. Surf Sci. 2008;602:2801–7.

56. Gaspar AB, Dieguez LC. Dispersion stability and methylcy-clopentane hydrogenolysis in Pd/Al$_2$O$_3$ catalysts. Appl Catal A-Gen. 2000;201:241–51.

57. Tessier D, Rakai A, Bozon-Verduraz F. Spectroscopic study of the interaction of carbon monoxide with cationic and metallic palladium in palladium–alumina catalysts. J Chem Soc Faraday Trans. 1992;88:741–9.

58. Ciuparu D, Bensalem A, Pfefferle L. Pd–Ce interactions and adsorption properties of palladium: CO and NO TPD studies over Pd–Ce/Al$_2$O$_3$ catalysts. Appl Catal B-Environ. 2000;26:241–55.

59. Nilsson PO. Optical properties of PdO in the range of 0.5–5.4 eV. J Phys C Solid State Phys. 1979;12:1423–7.